Superconductor Science and Technology

PAPER • OPEN ACCESS

Penetration depth of shielding currents due to crossed magnetic fields in bulk (RE)-Ba-Cu-O superconductors

To cite this article: J Srpi *et al* 2019 *Supercond. Sci. Technol.* **32** 035010

OPEN ACCESS
IOP Publishing
Superconductor Science and Technology
Supercond. Sci. Technol. **32** (2019) 035010 (14pp)
https://doi.org/10.1088/1361-6668/aafcd3

Penetration depth of shielding currents due to crossed magnetic fields in bulk (RE)-Ba-Cu-O superconductors

J Srpčič[1,3], F Perez[1], K Y Huang[1], Y Shi[1], M D Ainslie[1], A R Dennis[1], M Filipenko[2], M Boll[2], D A Cardwell[1] and J H Durrell[1]

[1] Bulk Superconductivity Group, Department of Engineering, University of Cambridge, Cambridge, CB2 1PZ, United Kingdom
[2] Siemens AG Corporate Technology eAircraft, Willy-Messerschmitt-Str. 1, D-82024, Taufkirchen, Germany

E-mail: js2308@cam.ac.uk

Received 25 October 2018, revised 14 December 2018
Accepted for publication 9 January 2019
Published 12 February 2019

Abstract

Exposure to time-varying magnetic fields causes shielding currents to flow beneath the surface of a superconductor up to a field-dependent penetration depth. In trapped field applications of bulk superconductors, in which the decay of trapped field due to external AC magnetic fields is caused by current redistribution (and not by helating and temperature rise), this penetration depth determines the degree of current redistribution in the superconductor and, in turn, the degree of decay of trapped field. In this study we propose and validate experimentally a model to explain the rate of decay of trapped field in a single grain bulk $GdBa_2Cu_3O_{7-\delta}$ (GdBCO) superconductor exposed to an AC magnetic field in a crossed-field configuration. The model is based on calculating the time dependence of the trapped field using the Biot–Savart law and assuming that the time dependence of the current density changes at the depth of penetration of the induced shielding currents. Inside the superconductor, where the crossed-field has not penetrated, the time dependence is assumed to be logarithmic and the decay of current density due to flux creep, whereas within the penetration depth of the surface the time dependence is assumed to be exponential and the decay of current density due to its redistribution. The penetration depth was measured separately using SQUID magnetometry and used as an input parameter to the model. The model was compared subsequently with measurements of the decay of trapped field and found to be in excellent agreement with the observed behaviour.

Keywords: bulk superconductors, AC loss, crossed-field decay, trapped field magnet, flux pinning

(Some figures may appear in colour only in the online journal)

Introduction

Flux creep, which is the random thermal activation of flux vortices from their pinning sites, is observed in the flux line lattice found in type-II superconductors and leads to a logarithmic decay of current density over time [1]. The rate of this decay can be approximated as

$$S = -\frac{\partial \log J}{\partial \log t} \approx \frac{k_B T}{U_0}, \quad (1)$$

where k_B is the Boltzmann constant, T is the temperature and U_0 is the pinning potential in the absence of any current, J. The rate of decay of the trapped magnetic field is expected to follow the same logarithmic time dependence as the current density, provided that the current does not change its

[3] Author to whom any correspondence should be addressed.

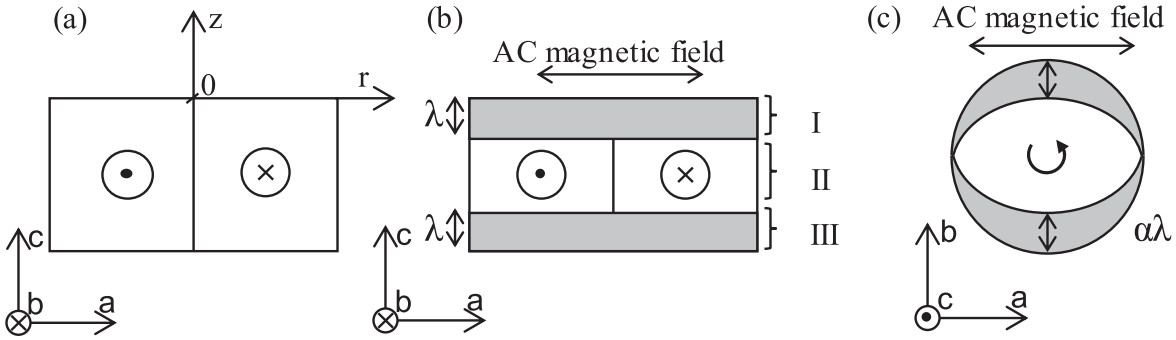

Figure 1. (a) Schematic illustration of the cross-section of a fully magnetised cylindrical bulk superconductor, in which the currents flow in the azimuthal direction. (b) The cross-section of a bulk superconductor after several cycles of AC magnetic field application (the orientation of the AC field is parallel the *a*-direction). The grey areas represent the penetration of shielding currents due to the AC magnetic field. The shielding currents are induced parallel or antiparallel to the *b*-direction during each half cycle of AC field. (c) Plan view of the penetration of shielding currents. Here, the currents flow in the *c*-direction, which means the penetration depth is larger than in (b) due to the lower critical current density in the *c*-direction.

direction. This is not the case, however, in the presence of external, time-varying magnetic fields that induce shielding currents to flow below the surface of the superconductor. This can cause the current density within the superconductor to be redistributed, leading, in turn, to decay of the trapped field. As an example, the trapped magnetic field of a fully magnetized bulk superconductor (i.e. a superconductor in which all flowing currents contribute constructively to the trapped magnetic field) will reduce, by definition, following any redistribution of current. As a result, external time-varying magnetic fields will lead to an accelerated rate of decay of trapped field.

Willemin *et al* [2] was the first to observe a strong shift in the irreversibility line in high-temperature superconductors caused by external AC magnetic fields applied perpendicular to the trapped magnetic field. This observation has been explained in terms of depinning of the flux vortices by the AC field, allowing them to move freely under the influence of the Lorentz force

$$\boldsymbol{F_L} = J \times B, \tag{2}$$

and escape the superconductor ($\boldsymbol{B}$ is the magnetic field density). The observed rate of decay was exponential across several orders of magnitude of trapped magnetic field.

Brandt and Mikitik [3] proposed an explanation for this behaviour for a thin-slab geometry, which was recently corroborated experimentally by Campbell *et al* [4]. The authors noted that the applied AC magnetic field alternately unpins parts of the flux vortices, trapped either near the top or bottom surfaces of the slab, enabling them to move in a stepwise manner in the direction of the Lorentz force during each completed half cycle of applied AC field. The decay of trapped field was found to be exponential over time in a fully penetrated superconducting slab.

Fagnard *et al* [5] investigated the decay of trapped field inside a bulk superconductor subjected to AC magnetic fields applied perpendicular to the direction of magnetization. They noted that, in such a configuration, shielding currents are induced from the top and bottom surfaces of the bulk sample up to a field-dependent penetration depth (see figure 1(b)). The decay of trapped field was investigated using the Biot–Savart law, assuming an initial full magnetization with a constant current density in the azimuthal direction flowing everywhere in the bulk superconductor, and subsequent reduction of the current density to zero in the region within the penetration depth of the surface. An upper bound to the decay, caused by the redistribution of shielding currents, is consequently established, although no explanation for the time dependence of current density has been given.

Bulk superconductors are technologically important materials due to their ability to trap high magnetic fields [6, 7]. The multitude of potential applications ranges from superconducting magnetic bearings, magnetic lenses, magnetic levitation, magnetic resonance imaging devices and drug delivery systems, to trapped field magnets in rotating machines, and possibly enabling technology for hybrid-electric passenger aircraft [8–14]. To date, the two main challenges to overcome before bulk superconductors can be applied widely are a practical means of magnetization (pulsed field magnetization shows great promise in that respect [15, 16]) and a way of mitigating trapped field decay (an ongoing field of research, both in the crossed-field [4, 17, 18] and in the parallel field configuration [19, 20]).

In this paper we present an analytical model in which the complete time dependence of trapped field of a bulk superconductor in the crossed-field configuration can be predicted accurately by virtue of knowing the critical current density of the superconductor and the sample geometry. The model combines the logarithmic and exponential time dependence of trapped field, which are characteristic of flux creep and crossed-field decay, respectively. This is achieved by assuming that the AC magnetic field causes the value of magnetization, averaged over a period of AC field, to approach zero exponentially in the penetrated region, and continuing logarithmic decay due to flux creep elsewhere. The time dependence of the trapped field is then calculated using the Biot–Savart law and compared to the results of experiment. Conversely, if the penetration depth is used as a fitting parameter, the model can be used to determine its value from measurements of trapped field decay.

Initially we present and outline the details of the analytical model and derive the time dependence of trapped field. We then derive a relation between the magnetization of a superconductor and the circulating currents for the case of an anisotropic critical current density distribution, which can be used to determine the anisotropy in critical current from magnetometry measurements. This is necessary information to determine the penetration of shielding currents in all directions in the sample. The experimental results of the AC decay measurements are presented and are shown to be in excellent agreement with predictions of the analytical model. Finally, the predictions of the analytical model are compared to those of a finite element model, which enables visualization of the shape of shielding regions in the superconductor and justifies the geometrical assumptions in the following section.

Analytical model

The model is based on calculating the trapped field on the surface of the bulk superconductor from the current density distribution $\boldsymbol{J}(\boldsymbol{r})$ inside the material using the Biot–Savart law

$$B(\boldsymbol{r}) = \frac{\mu_0}{4\pi}\iiint \frac{\boldsymbol{J}(\boldsymbol{r}') \times (\boldsymbol{r} - \boldsymbol{r}')}{|\boldsymbol{r} - \boldsymbol{r}'|^3} d^3\boldsymbol{r}'. \tag{3}$$

A distinct time dependence of the current density is assumed, depending on whether the current is flowing within the penetration depth of the AC magnetic field.

A schematic cross-section of the superconductor is shown in figure 1.

Figure 1(a) shows the cross-section of a fully magnetised bulk superconductor, in which the current circulates in the azimuthal direction. Assuming a constant current density, J_C, throughout the bulk superconductor as described by the Bean model [21], the induced magnetic field at the centre of the top surface can be written as [5, 22]

$$\begin{aligned} B &= \frac{\mu_0 J_C}{2}\int_0^R dr \int_{-h}^0 dz \frac{r^2}{\sqrt{(r^2+z^2)^3}} = \frac{\mu_0 J_C}{2} h \\ &\ln\left(\frac{R}{h} + \sqrt{1+\left(\frac{R}{h}\right)^2}\right) = \frac{\mu_0 J_C}{2} h f\left(\frac{R}{h}\right), \end{aligned} \tag{4}$$

where μ_0 is the permeability of free space, R and h are the radius and height of the bulk, respectively, r is the radial and z is the vertical coordinate. Here, it is convenient to define the function

$$f(x) = \ln(x + \sqrt{1+x^2}), \tag{5}$$

which will be used in the following analysis for purposes of clarity (equation (5) is equivalent to equation (2) in [22]). The constant J_C in equation (4) may be substituted by its time dependence (for example, a logarithmic time dependence in the case of flux creep), which leads, in turn, to a time dependence of trapped field $B(t)$.

Figure 1(b) shows the current density distribution within the cross-section of the bulk superconductor after the application of several cycles of AC magnetic field in the crossed-field configuration. The magnetic field penetrates into the bulk material from the top and bottom surfaces up to a penetration depth, λ, similarly to what is described in [5]. Figure 1(c) shows the schematic plan view of the penetration of shielding currents in the c-direction, induced by the applied AC magnetic field. Here, the thickness of the shielding regions is $\alpha\lambda$, where α is the critical current anisotrophy, as discussed below.

The AC magnetic field divides the bulk superconductor into three distinct regions along its height, each with a distinct time dependence of current density, depending on whether the current flows within the penetration depth of the surface. In region II, which is beyond the region penetrated by the AC magnetic field, the main mechanism of decay is via intrinsic flux creep, and the current density decays logarithmically with time as follows;

$$J = J_C\left(1 - k\ln\frac{t}{t_1}\right), \tag{6}$$

where J_C is the Bean critical current density, k is the logarithmic rate of decay, and t_1 is the time at which the AC field is turned on, so that $J(t = t_1) = J_C$.

In regions I and III, as well as within the periphery of the bulk superconductor (indicated by the shaded regions in figures 1(b) and (c)), the AC magnetic field acts to unpin the flux vortices, leading therefore to a redistribution of current density as the main mechanism of decay. The time dependence of current density is exponential,

$$J = J_C\exp\left(-\frac{t - t_1}{\tau}\right), \tag{7}$$

where τ is a characteristic time constant of decay. More accurately, it is not the current density J, that decays exponentially with time, instead it is the absolute value of the cross product $\boldsymbol{J}(\boldsymbol{r}') \times (\boldsymbol{r} - \boldsymbol{r}')$ (equation (3)), averaged over one period of AC field and integrated over the volume of the shielding region. This equivalence can be made since we are interested ultimately in the contribution of $\boldsymbol{J}(r')$ to the trapped field $\boldsymbol{B}(\boldsymbol{r})$. In addition, the choice of equation (7), although justified experimentally, is simply an approximation, and no derivation of this is presented here.

For simplicity of calculation, we assume that regions I and III are cylinders of radius R and height λ (both axes in the plane of the page). Between them lies region II, which is again cylindrical and of radius $R - \alpha\lambda$ and height $h - 2\lambda$, but enveloped with the region of shielding currents in the c-direction of the same height, outer diameter R and thickness $\alpha\lambda$. The factor α is introduced because the penetration depth of shielding currents in the c-direction differs from that of the currents in the ab-plane due to the different value of critical current density that results from anisotropy of the bulk superconductor. Here, a value of $\alpha = 3$ is assumed, which was corroborated by direct measurements of the anisotropy in critical current described below (at self-field the critical current anisotropy was found to be $J_C^{ab}/J_C^c = 3$, which is consistent with previous studies [5]).

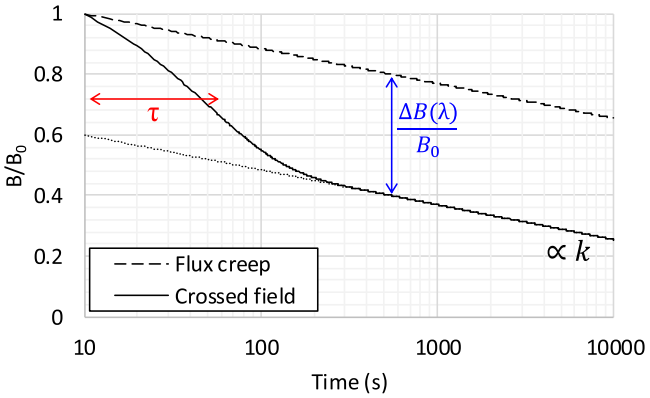

Figure 2. Graphical representation of equation (8) in a logarithmic plot (abscissa axis). The initial rate of decay is determined by the relaxation time τ, which is assigned to be 50 s in this representation. The rate of decay after several τ is determined by k, which is assumed to be 0.05. The total amount of decay due to current redistribution is determined by λ.

The time dependence of the trapped field can be obtained by substituting equations (6) and (7) into equation (3) and integrating to give

$$B(t) = \frac{\mu_0 J_C}{2}\left\{\begin{array}{c}\exp\left(-\dfrac{t-t_1}{\tau}\right)\left[h f\left(\dfrac{R}{h}\right) - (h-\lambda) f\left(\dfrac{R-\alpha\lambda}{h-\lambda}\right) + \lambda f\left(\dfrac{R-\alpha\lambda}{\lambda}\right)\right] \\ + \left(1 - k\ln\dfrac{t}{t_1}\right)\left[(h-\lambda) f\left(\dfrac{R-\alpha\lambda}{h-\lambda}\right) - \lambda f\left(\dfrac{R-\alpha\lambda}{\lambda}\right)\right]\end{array}\right\}. \quad (8)$$

The terms in square brackets are constant for a given bulk geometry and penetration depth, which makes equation (8) simply a weighted sum of an exponential and logarithmic function. The shape of the time dependence (compared to that of flux creep) is shown in figure 2.

The parameter τ, which is a time constant, determines the initial rate of decay of trapped field due to the exponential decay of current density in regions I and III. The parameter k determines the rate of decay $\partial \ln J/\partial \ln t$ at a time $t \gg \tau$ and is related to the pinning potential of the superconductor; in the case of flux creep $k = S = k_B T/U_0$. The parameter λ is the penetration depth of the shielding currents and determines the total decay of trapped field, $\Delta B(\lambda)/B_0$, beyond that due to flux creep (see figure 2). The parameters k, τ and λ may all depend on the amplitude and frequency of the applied magnetic field, as well as on the operating temperature of the superconductor. Here, we assume isothermal conditions, i.e. the temperature rise due to the heat generated by the movement of flux vortices is negligible. All three parameters represent measurable quantities and can be, if known, used as inputs to the model. Conversely, they can be used as fitting parameters and compared to their measured values in order to establish the validity of the model.

The decay $\Delta(\lambda)/B_0$ depends on the geometry of the bulk superconductor (i.e. the aspect ratio of the single grain, $\eta = R/h$), as shown in figure 3(a). The decay is calculated from the ratio between the field induced by the current in region II, shown in figures 1(b) (i.e. the second term in square brackets of equation (8), without the time dependence factor), and the induced field of a fully magnetised bulk superconductor, in equation (4). This can be used as an estimate of the decay of trapped field following the initial redistribution of circulating current, after which equilibrium is reached.

The decay for all values of η is equal to zero when $\lambda = 0$ and is complete when the shielding currents penetrate to the centre of the bulk superconductor. The shielding currents for a value of $\eta = 1.5$ reach the centre simultaneously from the top and bottom surfaces and from the outside edge (the value of 1.5 is due to the value of the critical current anisotropy of 3). For the cases in which $\eta > 1.5$ the decay becomes complete when $\lambda = h/2$, whereas when $\eta < 1.5$ the decay is complete when $\lambda = R/3$.

The effect of the aspect ratio, η, on decay is related directly to the evaluation of the trapped field at the top surface of the bulk superconductor. The current redistribution for bulk samples with a small value of η ($h \gg R$) displaces the active volume, contributing to the trapped field, away from the top surface (the active volume is region II in figure 1(b)). Since most of the currents flow close to the geometrical axis of the bulk superconductor, the distance between the active area and the top surface will be approximately λ. Conversely, in bulk materials with a large value of η ($R \gg h$), the current can flow at a large radius, $R \gg \lambda$, which will increase to a distance $\sqrt{\lambda^2 + R^2} \approx R$ from the centre of the top surface following the current redistribution. As a result, the decay of trapped field will be larger for bulk superconductors with a lower value of η and will approach $2\lambda/h$ as $\eta \to \infty$.

This result can be compared with the optimal value of aspect ratio, η, at which the trapped field on the surface of the bulk superconductor is highest. Rewriting equation (4) in terms of η, the trapped field on the top surface of a fully magnetised bulk becomes

$$B = \frac{\mu_0 J_C R}{2}\frac{f(\eta)}{\eta}, \quad (9)$$

where the factor $f(\eta)/\eta$ is unity for $\eta = 0$ and decreases with increasing η [22]. This seemingly favours a very different aspect ratio to that described above, as $\eta \to \infty$ leads to the lowest rate of decay due to the presence of crossed-fields.

However, while increasing the bulk sample height for a given radius and a given penetration depth leads to a lower aspect ratio η, it also leads to a lower ratio λ/h, and therefore to a lower decay overall (decreasing λ/h is equivalent to moving to the left in the graph in figure 3(a), in which direction the decay decreases). Therefore, for a given radius and penetration depth, increasing the height of the bulk sample indeed leads to a larger initial trapped field and to a lower rate of decay due to the redistribution of current. The latter effect is shown in figure 3(b).

Fitting equation (8) to measurements of the decay of trapped field in the crossed-field configuration provides insight into the relationship between the parameters τ, λ and k, and the amplitude and frequency of the applied AC magnetic field. As an example, after a long time ($t \gg \tau$) of the application of AC field to the bulk superconductor, the decay in trapped field beyond that associated with flux creep is determined solely by the penetration depth λ of the magnetic field (provided that the rate of decay k is the same for flux creep and decay due to the crossed-field). Independent measurements of λ could, therefore, serve as a predictor of the decay of trapped field at longer times.

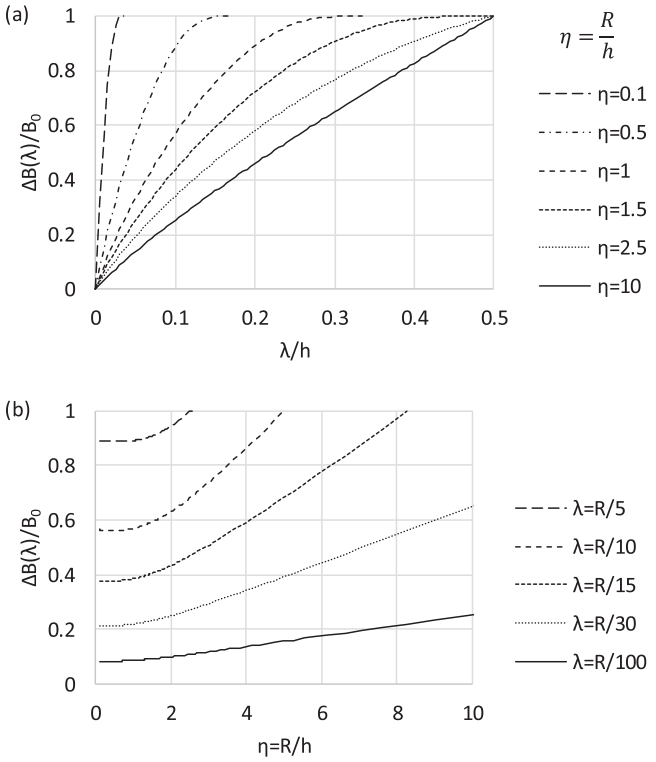

Figure 3. (a) The dependence of the decay of trapped field due to current redistribution on penetration depth λ for different values of the bulk superconductor aspect ratio $\eta = R/h$. (b) The decay of trapped field as a function of aspect ratio for different values of penetration depth.

Measurement of critical current anisotropy with magnetometry techniques

The external magnetic field is applied typically in the crystallographic c-direction of the bulk superconductor in field-cooled experiments of GdBCO, so that the shielding currents are induced in the ab-plane, in which the critical current density is highest [23], leading to the highest trapped field. In such cases it is sufficient to know the $J_C(B)$ dependence in the ab-plane to calculate the penetration depth, the penetration field and the achievable peak trapped field.

In the crossed-field configuration, however, the orientation of the external AC magnetic field is applied perpendicular to the trapped field and parallel to the ab-planes. In this case, the shielding currents are induced both in the ab-plane and in the c-direction in order to complete the current loops. This means that, when analyzing the crossed-field configuration, the current density in the c-direction must be known in order to predict the penetration of shielding currents in all directions. Here, we present a convenient way of deducing the critical current anisotropy from measured $M(B)$ loops where the direction of magnetic field is perpendicular to the c-direction.

Magnetometry is a common technique used to measure the $J_C(B)$ characteristic indirectly [24]. This involves calculating $J_C(B)$ from the measured $M(B)$ loop of a given sample using the following equation [25]

$$J_C(B) = \frac{\Delta M(B)}{a\left(1 - \frac{a}{3b}\right)}, \tag{10}$$

where $\Delta M(B) = M_-(B) - M_+(B)$ is the difference between the magnetization during ramp down and ramp up of the external magnetic field, B, respectively, and $2a$ and $2b$ ($a < b$) are the dimensions of the sample cross-section. Equation (10) assumes a constant, isotropic J_C and full field penetration of the bulk superconductor.

To derive a more general formula for the case of an anisotropic J_C, we follow a procedure outlined in [26] to obtain the relation between the magnetization of a sample and the circulating currents within. The basis of the calculation is illustrated schematically in figure 4.

The sample dimension is assumed to be infinite in the z-direction, with a cross-section of $2b \times 2c$ in the xy-plane. The critical current density in the x-direction is J_B and J_C in the y-direction. Assuming full field penetration, the current distribution falls into four regions across the sample cross-section, in each of which the current has a different direction. In the isotropic case of $J_B = J_C$ and with $b = c$, these four regions are described by identical isosceles triangles, rotated by an angle $\theta = 45°$ around the centre of the cross-section. If $b \neq c$, however, two of the triangles are extended into isosceles trapezoids with the same angle θ. Finally, by introducing the anisotropy $J_B \neq J_C$, θ must change in accordance with the condition $\nabla \cdot \boldsymbol{J} = 0$ (i.e. no current sources within the sample). From figure 4(a), this means $J_C\, b = J_B\, b \tan\theta$, leading to

$$\tan\theta = \frac{J_C}{J_B}. \tag{11}$$

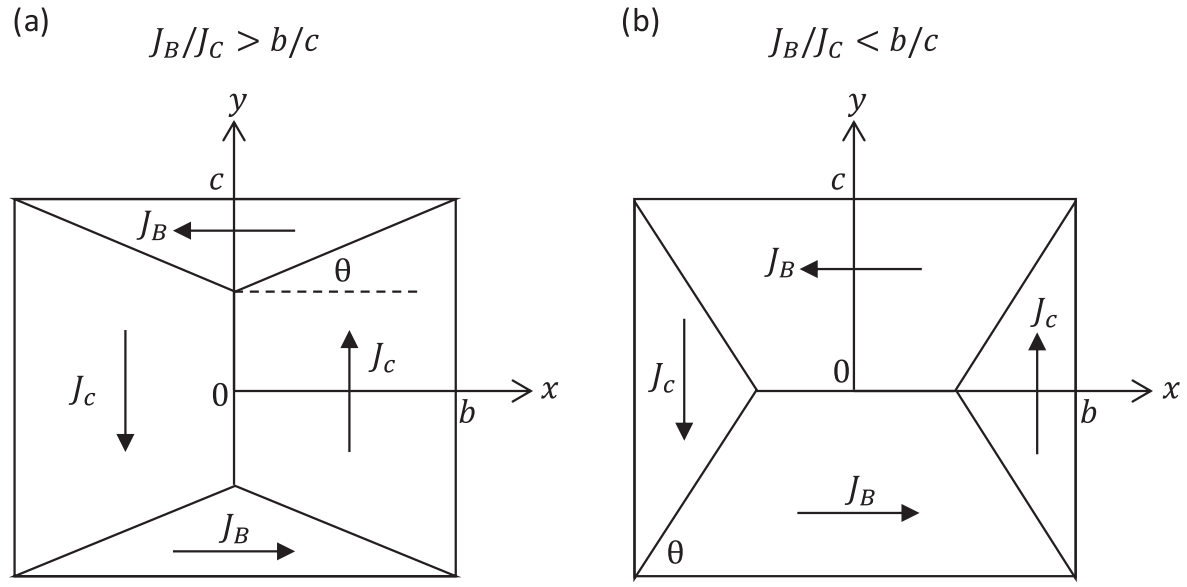

Figure 4. The distribution of current density in the *bc*-plane when the current density distribution is anisotropic. In (a) $J_B/J_C > b/c$ and in (b) $J_B/J_C < b/c$.

The local magnetisation can then be calculated from the current distribution via $\nabla \times \boldsymbol{M} = \boldsymbol{J}$, with the added constraint of $\boldsymbol{M} = 0$ at the boundary. The total magnetisation can be calculated subsequently as the average of the local magnetisation across the entire sample cross-section. Only the region ($x > 0$, $y > 0$) has to be considered in the calculation due to the symmetry of the arrangement (illustrated in figure 5).

The local magnetisation in the z-direction can be determined from the current distribution $J_C \hat{e}_y$ in region I and $-J_B \hat{e}_x$ in region II (where $\hat{e}_x$ and $\hat{e}_y$ are the unit vectors in the x- and y-direction, respectively) as

$$\begin{aligned} M^I(x) &= J_C(b - x), \quad \text{region I}, \\ M^{II}(y) &= J_B(c - y), \quad \text{region II}. \end{aligned} \tag{12}$$

The boundary separating regions I and II is a straight line

$$y(x) = J_C/J_B(x - b) + c. \tag{13}$$

The total magnetisation can then be expressed as an average value

$$M = \frac{1}{bc}\int_{I,II} (M^I(x')\, y' dx' + M^{II}(y')\, x' dy'). \tag{14}$$

Substituting equation (12) and $dy'/dx' = \tan\theta = J_C/J_B$ into equation (14) yields a one-dimensional integral. The result can then be expressed as

$$\Delta M = \begin{cases} J_C\, b \left(1 - \dfrac{J_C}{J_B}\dfrac{b}{3c}\right), & J_B/J_C > b/c, \\ J_B\, c \left(1 - \dfrac{J_B}{J_C}\dfrac{c}{3b}\right), & J_B/J_C < b/c, \end{cases} \tag{15}$$

which reduces to equation (75b) in [25] for the case of $J_B = J_C$ (to calculate the case $J_B/J_C < b/c$ one can simply substitute $b \leftrightarrow c$ and $J_B \leftrightarrow J_C$). $J_C(B)$ can then be extracted from $M(B)$ measurements by inverting the field dependence

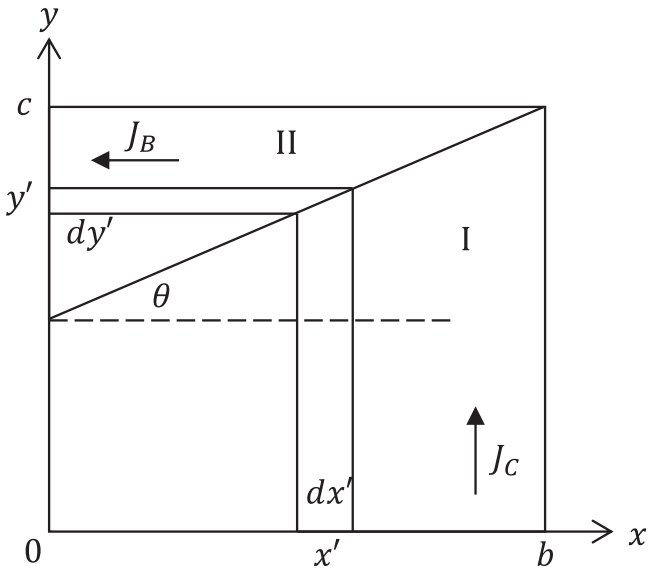

Figure 5. Illustration of the schematic of integration. The surface element is $x'dy' + y'dx'$ (the area of the 'L'-shaped region) and the integration limits are $x' = 0$ and $x' = b$.

of current density in equation (15), as follows

$$J_C = \begin{cases} \dfrac{3c}{2b}J_B - \sqrt{\left(\dfrac{3c}{2b}J_B\right)^2 - \dfrac{3c}{b^2}J_B\,\Delta M}, & J_B/J_C > b/c, \\ \dfrac{c}{3b}J_B\left(1 - \dfrac{\Delta M}{J_B\, c}\right)^{-1}, & J_B/J_C < b/c. \end{cases} \tag{16}$$

It is not possible to deduce the $J_C(B)$ characteristic from $M(B)$ loop measurements without knowing the $J_B(B)$ characteristic beforehand (and vice versa), since the magnetization depends on both J_B and J_C. However, the second term in the brackets in equation (15) depends on the ratio b/c of the

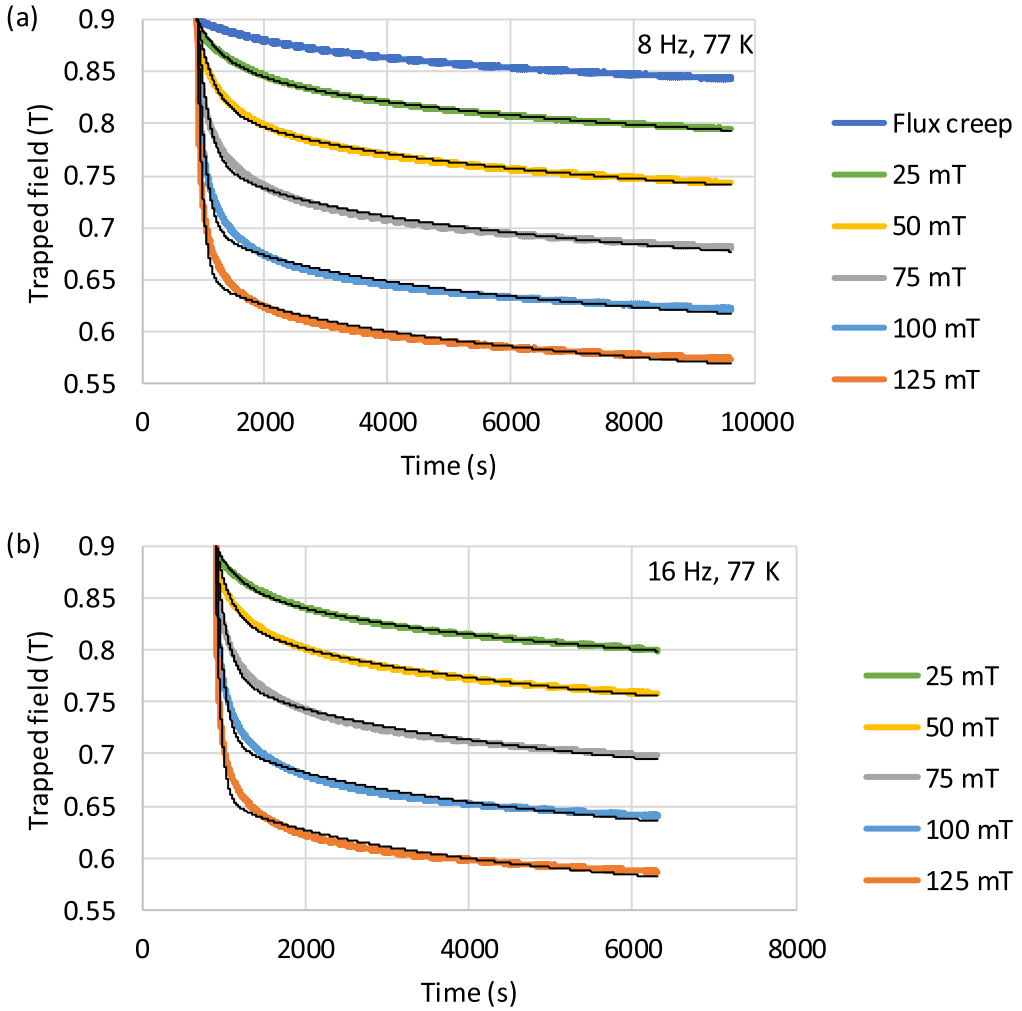

Figure 6. Measurement of trapped field during the application of an external AC magnetic field of various amplitudes at frequencies of (a) 8 Hz and (b) 16 Hz. The black lines represent the results of the analytical model with the fitting parameters listed in table 1.

dimensions of the sample cross-section, so, if the sample shape is chosen so that $c \gg b$ (and assuming $J_B \approx J_C$), equation (16) reduces to

$$\Delta M = J_C\, b, \tag{17}$$

which is the expression for the magnetization of an infinite slab, carrying a current J_C. As a result, equation (17) can be used to obtain the critical current density from magnetization loop measurements with a relative error of $\sim b/3c$.

It should be pointed out that it is not possible to use the $J_B(B)$ characteristic, measured in the isotropic case, to calculate $J_C(B)$ using equation (16). Although the current J_B flows in the *ab*-planes both in the isotropic and the anisotropic case, the underlying microscopic picture is quite different. In the isotropic case the flux vortices are pinned perpendicular to the *ab*-planes, while in the anisotropic case they are pinned within the *ab*-planes. This leads to fundamentally different behaviour, and most notably in the different values of the irreversibility field, which increase greatly when the vortices are pinned within the *ab*-planes (see the results section, below).

Experimental

A $GdBa_2Cu_3O_{7-\delta}$ bulk superconductor of diameter 30 mm and thickness 6 mm with added silver (10 wt%) fabricated by the top-seeded melt growth technique (TSMG) [27, 28] was used in this study. This was produced by cutting in half an as-grown sample of dimensions 30 mm in diameter and 12 mm thickness along the *ab*-plane. The top half was used for the measurements of AC decay and the bottom half for the characterization of the $J_C(B)$ dependence using SQUID magnetometry.

The bulk superconductor was field cooled in a liquid nitrogen bath in 1.5 T generated by an electromagnet with a magnetic field ramp-down rate of 0.015 T s^{-1}. The trapped field was allowed to undergo flux creep for a period of 900 s following magnetization, after which the trapped field at the centre of the bulk sample was observed to be 0.9 T with a conical profile, indicating full magnetisation. Subsequently, the bulk superconductor was inserted into the bore of a solenoid coil, which itself was submerged in liquid nitrogen, and exposed to several thousand cycles of AC magnetic field. The solenoid was connected to an AC current source with a

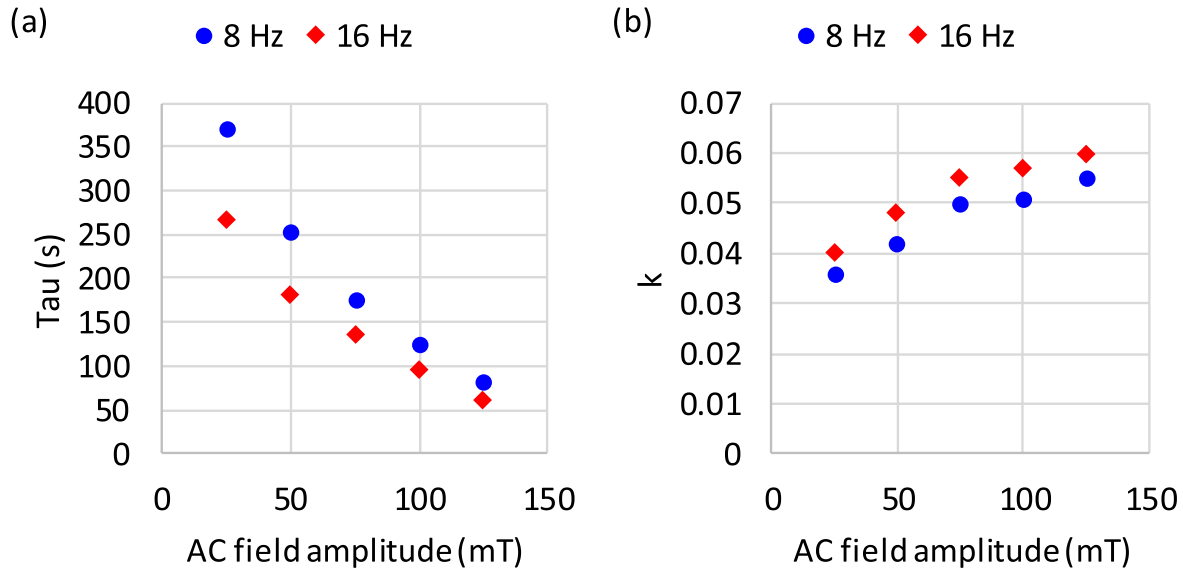

Figure 7. Values of the fitting parameter τ (a) and k (b).

maximum current of 40 A to generate the magnetic field, with a maximum amplitude of 250 mT. The trapped field of the bulk superconductor was measured using a calibrated Hall sensor mounted on the centre of its top surface.

The temperature of the bulk superconductor during the application of the AC magnetic field was monitored using a Cernox® temperature sensor, also mounted on the top surface of the sample (but several millimetres from the centre) with Apiezon N cryogenic vacuum grease. The bulk was placed into the bore of the solenoid coil in a non-magnetised state and exposed to 60 s of applied AC magnetic field, at which point the temperature was found to stabilize for all AC magnetic field amplitudes and frequencies.

Two cuboid samples were cut out of the bottom half of the as-grown sample for magnetometry measurements. The first, of dimensions $a = 2.85$ mm, $b = 2.75$ mm and $c = 5.65$ mm, was placed into the SQUID magnetometer with the external magnetic field applied along the sample c-direction. The $M(B)$ loop was then measured in an applied external magnetic field of up to $B = 5$ T, from which the $J_C(B)$ characteristic was deduced using equation (10) (i.e. for the value of J_C in the ab-plane).

The second sample had dimensions $a = 4.7$ mm, $b = 1.18$ mm and $c = 5.6$ mm, and was placed into the SQUID magnetometer with the external magnetic field applied along the a-direction. The measured $M(B)$ loop was used to deduce the $J_C(B)$ characteristic in the c-direction using equation (17). The error in the estimate of J_C, given by the ratio of the dimensions of the sample cross-section, was $b/3c = 7\%$.

Numerical modelling framework

Finite element modelling was performed using the commercial software package Comsol Multiphysics 5.3a, and based on the $\boldsymbol{H}$-formulation for 2D, infinitely long slab geometry [29]. Ampere's and Faraday's laws are solved in this framework in conjunction with a constitutive relation between the electric field, E, and the current density, J. Here, the power law $E = E_0(J/J_C)^N$ was assumed, where $E_0 = 1\ \mu\text{V cm}^{-1}$, $N = 20$ and $J_C = 2.6 \times 10^8\ \text{A m}^{-2}$. The critical current density was assumed to be constant and its value was chosen so that the simulated trapped field was consistent with the experimental data. The temperature was assumed to be constant at 77 K, so no thermal model was employed. The slab geometry was set to be 30 mm wide and 6 mm thick in order to match the dimensions of the bulk superconductor characterised experimentally.

Table 1. The values of fitting parameters τ, k and λ for the analytical model (the black curves in figure 6).

	8 Hz			16 Hz		
Amplitude	τ (s)	k	λ (mm)	τ (s)	k	λ (mm)
25 mT	372	0.036	0.042	266	0.040	0.043
50 mT	252	0.042	0.114	181	0.048	0.098
75 mT	175	0.050	0.216	136	0.055	0.198
100 mT	125	0.051	0.350	96	0.057	0.324
125 mT	84	0.055	0.455	61	0.060	0.447

Results

Two sets of measurements of trapped field decay at two different frequencies and various amplitudes of applied AC magnetic field are shown in figure 6. Also shown (black lines) is the fitted analytical model, with all the values for the respective parameters τ, λ and k listed in table 1. The temperature rise was at most 0.2 K for all the applied AC magnetic field amplitudes and frequencies, validating the isothermal assumption in the derivation of the model.

The trapped field of the bulk superconductor decays significantly in the first ~1000 s after the start of AC field

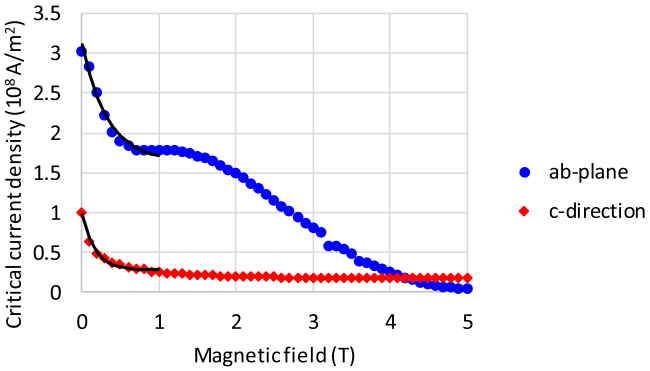

Figure 8. The measured critical current density in the *ab*-plane (blue) and in the *c*-direction (red). The black lines represent fits of an exponential function, used to calculate the penetration depth.

application in all cases, after which the rate of decay decreases markedly and approaches that of flux creep. This behaviour, with two distinct regions of greatly differing decay rate, is characteristic of crossed-field decay and has been observed previously [5]. The crossover time between the two regions is determined primarily by the parameter τ, which is illustrated graphically in figure 7(a).

The decay rate of trapped field normalised to the period of the AC field should be independent of frequency within the framework of the Bean model. This implies that, at a given amplitude of AC magnetic field, the value of τ at 8 Hz should be twice the value of τ at 16 Hz. The relative variation of τ, extracted from our decay measurements, is ∼1.3–1.4 times for all amplitudes of AC field (see table 1). Given that the analytical model assumes a number of simplifications, this result is not too far from the value, predicted by Bean's critical state model. A possible explanation for the slight discrepancy (here purely speculative) could be due to the AC magnetic field causing the value of magnetisation, averaged over a period of AC field and over the volume of penetration, to behave effectively as if it were in the reversible regime. Then, the movement of flux vortices is determined by the Lorentz force (in the absence of flux pinning the current density is proportional to the electric field [30], leading to exponential decay). However, some frequency dependence remains since not all the flux vortices necessarily enter the reversible regime (since the pinning force is distributed over a range of values and some vortices may be pinned in place more strongly than others [31]).

The dependence of the parameter k on the AC magnetic field amplitude is shown in figure 7(b). The value of this parameter determines the rate of decay in the steady state, and when the shielding currents have all been redistributed and the main mechanism of decay is flux creep. It is shown that the value of k increases with amplitude at both frequencies. Although the nature of logarithmic decay is such that the rate of decay is inversely proportional to the time elapsed (suggesting a convergence of the rate of decay to that of flux creep), the value of k may still differ for different values of the AC magnetic field amplitude. This may be explained by the local penetration of the AC magnetic field, which causes a reduction in the critical current density proportional to the amplitude. In turn, the superconductor can no longer support the established trapped field profile in the periphery. As a result, an AC magnetic field of a greater amplitude will lead to a greater rate of decay of trapped field.

It is possible that the model overestimates the values of k, as evidenced by the slight discrepancy of the rate of decay between the model and experiment for times $t \gg \tau$. This is simply due to the analytical least-square fit being optimised to minimise the difference between the analytical solution and the data, rather than between their respective derivatives. The optimal way of mitigating this possible error would be to measure the values of k in a separate experiment and use these as inputs to the analytical model. However, this is beyond the scope of the present work.

The critical current characteristic of the sample was measured indirectly by magnetometry to compare the values of penetration depth predicted by the analytical model and measured values, with the result shown in figure 8. The critical current density was measured in a magnetic field of up to 6 T, although the analysis presented here can be limited to fields up to 1 T, since neither the trapped field, nor the AC magnetic field amplitude exceed this value. The critical current density in the interval (0, 1 T), was fitted with an exponential function, which was used subsequently to calculate the penetration depth using the modified Bean model.

The following fitting function was used for the $J_C(B)$ data;

$$J_C(B) = J_1 + J_2 \exp\left(-\frac{B}{B_1}\right), \tag{18}$$

where the parameters for the critical current density in the *ab*-plane are $J_1 = 1.65 \times 10^8$ A m^2, $J_2 = 1.46 \times 10^8$ A m^2, $B_1 = 0.32$ T and for the critical current in the *c*-direction are $J_1 = 0.27 \times 10^8$ A m^2, $J_2 = 0.70 \times 10^8$ A m^2, $B_1 = 0.19$ T. The exponential functions are represented as black curves in figure 8 up to a value of magnetic field of 1 T. The penetration depth can be calculated by substituting equation (18) into Ampere's law, $\nabla \times \boldsymbol{B} = \mu_0 \boldsymbol{J_C}(\boldsymbol{B})$, and integrating from 0 to the amplitude of the external magnetic field, B_0. Solving for B gives the field profile inside the bulk superconductor,

$$B(z) = B_1 \cdot \log\left(\frac{\left(J_1 + J_2 \cdot \exp\left(-\frac{B_0}{B_1}\right)\right) \cdot \exp\left(\frac{B_0 - J_1 \mu_0 z}{B_1}\right) - J_2}{J_1}\right), \tag{19}$$

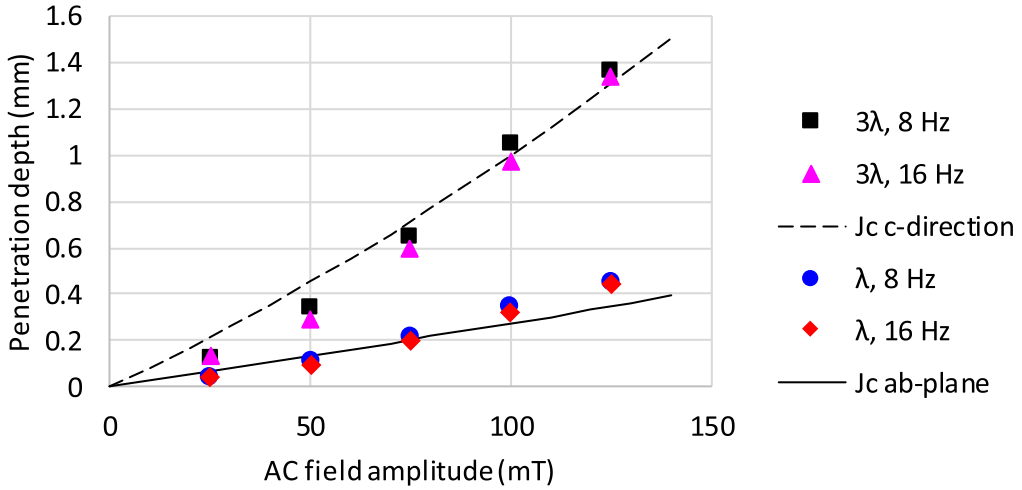

Figure 9. The values of penetration depth, obtained by fitting the analytical model to the experimental data (symbols), compared with the values calculated from the measured $J_C(B)$ dependence (lines). The values of 3λ are compared to the penetration depth of shielding currents in the c-direction assuming a critical current anisotropy value $\alpha = 3$.

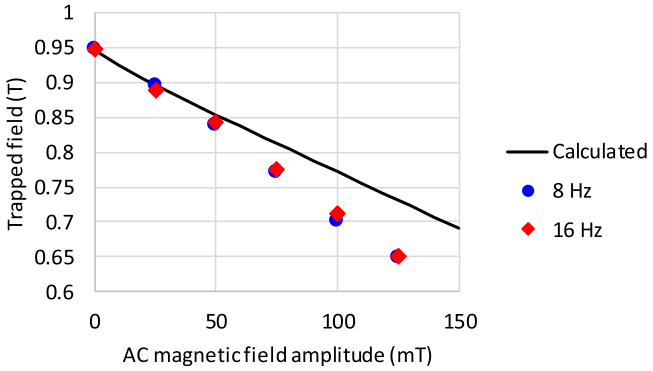

Figure 10. The predicted value of decay of trapped field (black line), compared to the experimental data. The data are taken 6300 s after the start of the application of AC magnetic field.

where z is the distance measured inwards from the surface of the superconductor. The penetration depth can then be obtained from equation (19) by substituting $B(z) = 0$ and solving for z, giving

$$\lambda = \frac{B_0 - B_1 \cdot \log\left(\dfrac{J_1 + J_2}{J_1 + J_2 \cdot \exp\left(-\dfrac{B_0}{B_1}\right)}\right)}{\mu_0 J_1}, \qquad (20)$$

which reduces to the Bean penetration depth for a constant J_C, $B_0/\mu_0 J_C$, by substituting $J_1 = J_C$ and $J_2 = 0$. This result can be compared with the values of λ, obtained by fitting the analytical model to experimental data, as shown in figure 9.

The values of penetration depth, obtained by fitting the analytical model to the data, appear to be in good agreement with the values calculated from the measured $J_C(B)$ dependence. Additionally, the choice in the value of the anisotropy factor of the critical current is justified, since the values of 3λ coincide with the penetration depth of shielding currents in the c-direction.

The penetration depth depends weakly on frequency at all amplitudes of AC magnetic field. However, the penetration depth appears lower at the higher frequency of 16 Hz than it does at 8 Hz, which is not accounted for by the analytical model given that the data in figure 9 represent the quasy-static limit $\omega \to 0$ (Bean model). It has been noted previously that the penetration depth does depend on frequency [19, 32], although the precise dependence is determined by the constitutive relation between the electric field and current density, which may be difficult to ascertain accurately (in the case of Ohm's law the proportionality is $\lambda \propto \omega^{-1/2}$).

The calculated values of penetration depth can be used as an input to the analytical model, which enables the decay of trapped field over time to be predicted. To this end, the factor $\Delta B(\lambda)/B_0$ can be calculated for the values of penetration depth given by equation (20). This yields the ratio of circulating currents before and after the redistribution of current due to application of the AC magnetic field. This factor can then be multiplied by the trapped field at a given time in the case where no AC magnetic field has been applied (in which the trapped field decay is due only to flux creep). This predicts the decay of trapped field as a function of penetration depth, which is compared with the results of experiment in figure 10.

The predicted value of field decay appears to be in reasonable agreement with experiment, given that the margin of error in determining the rate of decay is less than 10%. The discrepancy arises because the analytical model overestimates slightly the value of penetration depth relative to the values given by the measured $J_C(B)$ characteristic (see figure 9). This disagreement can be explained within the context of the analytical model being mathematically ideal with well-defined regions of shielding current, which is only an approximation of the real behavior. In reality, the initial state of a fully magnetised superconductor may have regions with current lower than J_C (or flowing in a different direction than that assumed) and, additionally, the geometries of the regions

of induced shielding will not be perfect cylinders and rings as assumed by the model. Additionally, the critical current density was measured from a specimen of the parent bulk superconductor cut from the bottom half of the as-grown, single grain sample. The measured data may not correspond to the true value of critical current density since this parameter is not necessarily constant throughout the volume of the sample (typically, its value decreases with increasing distance from the seed crystal).

However, the analytical model describes the experiment remarkably well despite the simplifications described above. This is true both in reproducing the time dependence of trapped field and extracting the values of penetration depth from the theoretical fit to the data, as well as in predicting the decay of trapped field based on the specific values of penetration depth used as inputs to the model.

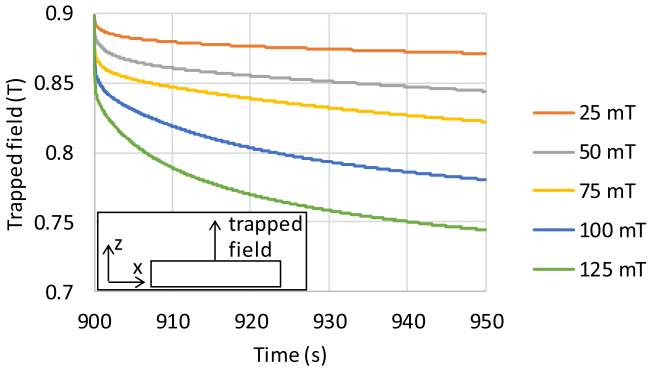

Figure 11. Simulated decay of trapped field for an AC field frequency of 8 Hz. Inset: the geometry of the superconductor modelled in this study. The dimension of the superconducting slab is assumed to be infinite in the direction perpendicular to the surface of the illustration (i.e. into the page).

Finite element modelling results

The geometry of the bulk superconductor modelled in this investigation is shown in the inset of figure 11. The dimensions of the superconducting slab were 30 mm in width by 6 mm in thickness, to match the cross-section of the measured bulk. The slab was magnetised initially in a zero field cooled process with the magnetic field applied in the y-direction. The magnetic field was ramped from 0 to 3 T over 150 s and subsequently ramped back to 0 at the same rate with the sample at 77 K. The superconductor was allowed to undergo flux creep for a period of 900 s, after which the external AC magnetic field was applied in the crossed-field configuration (i.e. parallel to the x-axis) at a frequency of 8 Hz and varying amplitude from 25 to 125 mT. The time dependence of trapped field, which was calculated 0.5 mm above the surface of the superconducting slab, is shown in figure 11.

The simulated and measured results are in good qualitative agreement (as evident from a comparison with the measured data in figure 6(a)), although there is some quantitative discrepancy between experiment and simulation. This can be attributed to the simplifications in the numerical model, such as the assumed 2D geometry, the field-independent and isotropic critical current density and an assumed ideal E–J power law behaviour.

The distribution of current density across the cross-section of the superconducting slab after ten applied cycles of AC magnetic field is shown in figure 12(a). The shielding currents are induced mainly from the top and bottom surfaces of the slab, which is consistent with the initial assumptions in the derivation of the analytical model. In addition, some shielding currents are induced from the side surfaces of the slab, related to the finite geometry, that might account for the overestimation of the penetration depth given by the fit of the analytical model to measured data. The distribution of current density beyond the penetration depth of the shielding currents appears not to be perturbed significantly by the application of the external AC magnetic field, the direction of which appears to remain unchanged, although its value decreases due to flux creep. This result corresponds to region II in the derivation of the analytical model (figure 1(b)).

The distribution of current density along height of the slab (the z-axis) is shown in figure 12(b). This data was taken from the middle of the left-hand side of the slab (7.5 cm from the centre) and shows clearly how the penetration depth of shielding currents increases with amplitude of the AC magnetic field. The value of the penetration depth we define as the location, at which the current changes sign (changes direction). The values of the penetration depth, obtained thus by FEM calculation are shown in figure 12(c) and compared with the analytical model and the calculated values from the critical current density. All three methods are in excellent agreement.

Discussion

We have shown that the analytical model is able to reproduce experimental data remarkably well for a multitude of different values of applied AC magnetic field amplitudes and frequencies. One of the main initial assumptions in the derivation of the model was that the superconductor is maintained under isothermal conditions, so that the critical current density, and, consequently, the penetration depth of shielding currents, does not change. However, since the AC magnetic field causes heat generation per unit volume, $Q = \boldsymbol{E} \cdot \boldsymbol{J}$, due to the dissipative movement of flux vortices, isothermal conditions may not be applicable for sufficiently large frequencies and amplitudes of applied AC magnetic field. It has been shown elsewhere that an AC magnetic field may generate sufficient heat to increase the temperature of the superconductor above the critical temperature (T_C) and lead to the total collapse of trapped magnetization [33].

We argue that the model is still valid with only some reconsideration of the initial assumptions in the advent of a temperature rise in the superconductor. If the cooling power of the cryogenic system is sufficient to prevent the temperature to rise above T_C, then eventually stationary conditions will be reached and the temperature will stabilize. At that

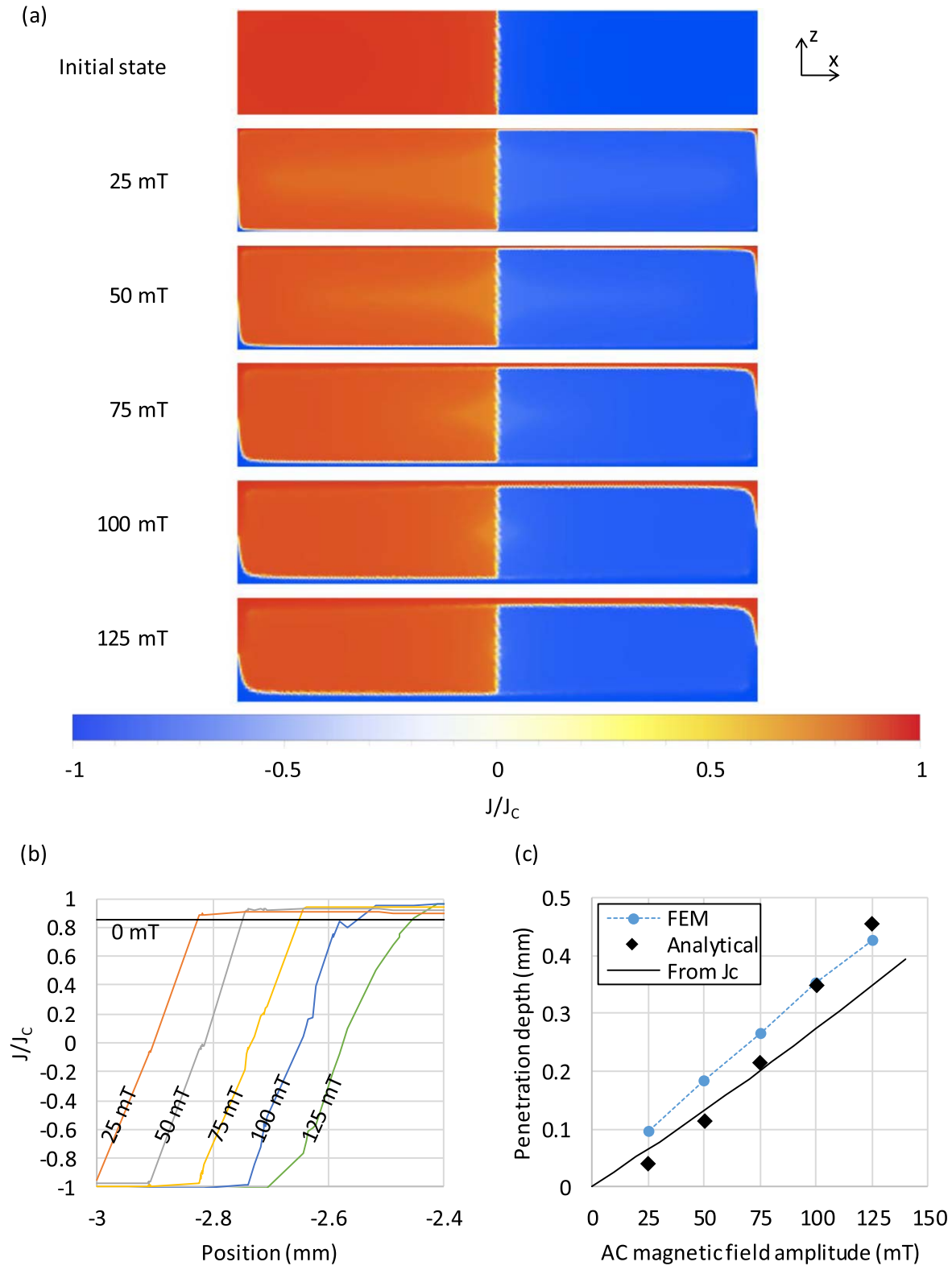

Figure 12. (a) The current density distribution in the superconducting slab after ten cycles of applied AC magnetic field at 8 Hz and at different amplitudes. (b) The current density distribution along the z-axis for all cases in (a). (c) The comparison of the penetration depth values given by the calculation from J_c (as in figure 9), by the analytical model an by FEM calculation.

point the temperature will not change any further, in which case isothermal conditions may, again, be assumed. The derivation of the model may proceed as above, provided the $J_C(B)$ characteristic at that temperature is known.

An estimate for how much the penetration depth changes, given a temperature rise, ΔT, can be obtained by comparing the heat generation per unit volume in the bulk, $Q = \boldsymbol{E} \cdot \boldsymbol{J}$, with the total heat that can be extracted from the

superconductor by the cooling system, Q_{OUT}. The temperature rise can be written as

$$\Delta T = \frac{\int \boldsymbol{E} \cdot \boldsymbol{J}\, dV - Q_{OUT}}{C}, \tag{21}$$

where C is the heat capacity of the superconductor. The change of the penetration depth can then be estimated as

$$\frac{\Delta\lambda}{\lambda} = -\frac{1}{J_C(T)}\left(\frac{\partial J_C}{\partial T}\right)\Delta T = -\frac{1}{J_C(T)}\left(\frac{\partial J_C}{\partial T}\right) \times \frac{\int E \cdot J\, dV - Q_{OUT}}{C}, \tag{22}$$

where $\left(\frac{\partial J_C}{\partial T}\right)$ represents the change in critical current density with temperature. The value of $\Delta\lambda$ can serve subsequently as an estimation of the error of the model, given a measured value of ΔT. In equation (22) both the heat capacity, C, and the thermal conductivity of the superconductor (which itself determines Q_{OUT}) are temperature dependent, and thus the value of $\Delta\lambda$ depends on both the AC magnetic field amplitude and frequency (which themselves determine the electric field, E), as well as the temperature of the superconductor.

The operating temperature of the superconductor in any practical rotating machine application is likely to be lower than 77 K, the frequency of the AC magnetic field be higher than 8 or 16 Hz and the trapped field of the superconductor higher than 0.9 T (the experimental parameters for the experimental data in this study). As an example, in potential aircraft applications the coolant of choice is likely to be liquid hydrogen (in the temperature range 20–30 K) and the frequency of external AC magnetic fields is likely to be in the range of 400–500 Hz [14]. At the lower temperature of 20 K, the heat capacity and the thermal conductivity of $GdBa_2Cu_3O_{7-\delta}$ are lower than at 77 K [34, 35]. Combined with a higher frequency of the AC magnetic field, this may lead to a higher temperature rise than that observed here at 77 K However, the higher J_C at the lower temperature will lead subsequently to a smaller volume in which heat is generated. Therefore, a thorough examination of the parameter space may be needed in which any potential application is expected to operate. We emphasize, however, that the analytical model presented here is sufficiently general that it can be modified easily to describe a different parameter space than that analysed in this study.

Conclusion

We have presented and validated experimentally an analytical model of trapped field decay in bulk superconductors due to an applied AC magnetic field in the crossed-field configuration. We have shown that, by assuming two distinct mechanisms of decay, current redistribution and flux creep, that the time dependence of trapped field in a bulk superconductor can be predicted within the Biot–Savart law. The body of the model consists of three fitting parameters, τ, λ and k, which can be used alternatively as input parameters in order to predict the decay of trapped magnetic field. We have shown further that the critical current density determines solely the amount of decay of trapped field in the stationary regime, in the absence of circulating current in the shielding regions. This is extremely useful since the $J_C(B)$ of a bulk superconductor can be measured routinely, from which the value of penetration depth can be determined and used as a predictor of field decay.

Acknowledgments

This work was supported by Siemens AG. The authors acknowledge the financial support from the Engineering and Physical Sciences Research Council (EPSRC) EP/P00962X/1. Dr Mark Ainslie would like to acknowledge financial support from an EPSRC Early Career Fellowship EP/P020313/1. We thank Professor Archie Campbell for very helpful discussions. All data are provided in full in the results section of this paper.

ORCID iDs

J Srpčič https://orcid.org/0000-0001-8195-4188
Y Shi https://orcid.org/0000-0003-4240-5543
M D Ainslie https://orcid.org/0000-0003-0466-3680
M Boll https://orcid.org/0000-0002-9778-4280
J H Durrell https://orcid.org/0000-0003-0712-3102

References

[1] Anderson P W 1962 Theory of flux creep in hard superconductors *Phys. Rev. Lett.* **9** 309
[2] Willemin M, Rossel C, Hofer J, Keller H, Erb A and Walker E 1998 Strong shift of the irreversibility line in high-Tc superconductors upon vortex shaking with an oscillating magnetic field *Phys. Rev.* B **58** R5940–3
[3] Brandt E H and Mikitik G P 2002 Why an ac magnetic field shifts the irreversibility line in type-II superconductors *Phys. Rev. Lett.* **89** 027002
[4] Campbell A, Baghdadi M, Patel A, Zhou D, Huang K Y, Shi Y and Coombs T 2017 Demagnetisation by crossed fields in superconductors *Supercond. Sci. Technol.* **30** 034005
[5] Fagnard J-F, Kirsch S, Morita M, Teshima H, Vanderheyden B and Vanderbemden P 2015 Measurements on magnetised GdBCO pellets subjected to small transverse ac magnetic fields at very low frequency: evidence for a slowdown of the magnetization decay *Physica* C **512** 42–53
[6] Durrell J H *et al* 2014 A trapped field of 17.6 T in melt-processed, bulk Gd-Ba-Cu-O reinforced with shrink-fit steel *Supercond. Sci. Technol.* **27** 082001
[7] Tomita M and Murakami M 2003 High-temperature superconductor bulk magnets that can trap magnetic fields of over 17 tesla at 29 K *Nature* **421** 517–20
[8] Matsunaga K, Tomita M, Yamachi N, Iida K, Yoshioka J and Murakami M 2002 YBCO bulk of the superconducting bearing for a 10 kWh flywheel *Supercond. Sci. Technol.* **15** 842–5

[9] Takahashi K, Fujishiro H and Ainslie M D 2018 A new concept of a hybrid trapped field magnet lens *Supercond. Sci. Technol.* **31** 044005
[10] Liao H, Zheng J, Jin L, Huang H, Deng Z, Shi Y, Zhou D and Cardwell D A 2018 Dynamic levitation performance of Gd–Ba–Cu–O and Y–Ba–Cu–O bulk superconductors under a varying external magnetic field *Supercond. Sci. Technol.* **31** 035010
[11] Nakamura T, Tamada D, Yanagi Y, Itoh Y, Nemoto T, Utumi H and Kose K 2015 Development of a superconducting bulk magnet for NMR and MRI *J. Magn. Reson.* **259** 68–75
[12] Nishijima S, Mishima F, Terada T and Takeda S 2007 A study on magnetically targeted drug delivery system using superconducting magnet *Physica* C **463–465** 1311–4
[13] Yamagishi K, Ogawa J and Tsukamoto O 2014 Rotation test of a superconducting bulk rotor shielded with superconducting rings *IEEE Trans. Appl. Supercond.* **25** 5201905
[14] Luongo A L, Masson P J, Nam T, Mavris D, Kim H D, Brown G V, Waters M and Hall D 2009 Next generation more-electric aircraft: a potential application for HTS superconductors *IEEE Trans. Appl. Supercond.* **19** 1055–68
[15] Fujishiro H, Tateiwa T, Fujiwara A, Oka T and Hayashi H 2006 Higher trapped field over 5T on HTSC bulk by modified pulse field magnetizing *Physica* C **445–448** 334–8
[16] Zhou D, Ainslie M D, Shi Y, Dennis A R, Huang K, Hull J R, Cardwell D A and Durrell J H 2017 A portable magnetic field of >3 T generated by the flux jump assisted, pulsed field magnetization of bulk superconductors *Appl. Phys. Lett.* **110** 062601
[17] Vanderbemden P, Hong Z, Coombs T A, Ausloos M, Hari Babu N, Cardwell D A and Campbell A M 2007 Remagnetization of bulk high-temperature superconductors subjected to crossed and rotating magnetic fields *Supercond. Sci. Technol.* **20** S174
[18] Fagnard J F, Morita M, Nariki S, Teshima H, Caps H, Vanderheyden B and Vanderbemden P 2016 Magnetic moment and local magnetic induction of superconducting/ferromagnetic structures subjected to crossed fields: experiments on GdBCO and modelling *Supercond. Sci. Technol.* **29** 125004
[19] Srpčič J *et al* 2018 Demagnetization study of pulse-field magnetized bulk superconductors *IEEE Trans. Appl. Supercond.* **28** 6801305
[20] Yamagishi K, Ogawa J, Tsukamoto O, Murakami M and Tomita M 2003 Decay of trapped magnetic field in HTS bulk caused by application of ac magnetic field *Physica* C **392–396** 659–63
[21] Bean C P 1962 Magnetisation of hard superconductors *Phys. Rev. Lett.* **8** 250
[22] Durrell J H, Dancer C E J, Dennis A, Shi Y, Xu Z, Campbell A M, Babu N H, Todd R I, Grovenor C R M and Cardwell D A 2012 A trapped field of >3 T in bulk MgB2 fabricated by uniaxial hot pressing *Supercond. Sci. Technol.* **25** 112002
[23] Fisher L M, Kalinov A V, Savel'ev S E, Voloshin I F and Yampol'skii V A 1998 Critical current anisotropy in YBCO superconducting samples *Physica* C **309** 284–94
[24] Namburi D K, Shi Y, Palmer K G, Dennis A, Durrell J H and Cardwell D A 2016 A novel, two-step top seeded infiltration and growth process for the fabrication of single grain, bulk (RE)BCO superconductors *Supercond. Sci. Technol.* **29** 095010
[25] Chen D X and Goldfarb R B 1989 Kim model for magnetization of type-II superconductors *J. Appl. Phys.* **66** 2489
[26] Peterson R L 1990 Magnetisation of anisotropic superconducting grains *J. Appl. Phys.* **67** 6930
[27] Shi Y, Namburi D K, Zhao W, Durrell J H, Dennis A and Cardwell D A 2016 The use of buffer pellets to pseudo hot seed (RE)–Ba–Cu–O–(Ag) single grain bulk superconductors *Supercond. Sci. Technol.* **29** 015010
[28] Zhou D, Hara S, Li B, Xu K, Noudem J and Izumi M 2013 Significant improvement of trapped flux in bulk Gd-Ba-Cu-O grains fabricated by a modified top-seeded melt growth process *Supercond. Sci. Technol.* **26** 015003
[29] Ainslie M D and Fujishiro H 2015 Modelling of bulk superconductor magnetization *Supercond. Sci. Technol.* **28** 053002
[30] Yeshurun Y, Malozemoff A P and Shaulov A 1996 Magnetic relaxation in high-temperature superconductors *Rev. Mod. Phys.* **68** 911–49
[31] Kiss T *et al* 2002 Distribution of pinning strength and scaling behavior in YBCO coated IBAD tape *Physica* C **382** 57–61
[32] Ueda H, Itoh M and Ishiyama A 2003 Trapped field characteristic of HTS bulk in AC external magnetic field *IEEE Trans. Appl. Supercond.* **13** 2283
[33] Ogawa J, Iwamoto M, Tsukamoto O, Murakami M and Tomita M 2002 Interaction between trapped magnetic field and AC loss in HTS bulk *Physica* C **372–376** 1754–7
[34] Fujishiro H, Yokoyama K, Kaneyama M, Oka T and Noto K 2004 Estimation of generated heat in pulse field magnetizing for SmBaCuO bulk superconductor *Physica* C **412–414** 646–50
[35] Fujishiro H, Katagiri K, Murakami A, Yoshino Y and Noto K 2005 Database for thermal and mechanical properties of REBaCuO bulks *Physica* C **426–431** 699–704